Orbital dilution effect in ferrimagnetic $Fe_{1-x}Mn_xCr_2O_4$: competition between anharmonic lattice potential and spin–orbit coupling

2010 J. Phys.: Condens. Matter 22 176003

(http://iopscience.iop.org/0953-8984/22/17/176003)

J. Phys.: Condens. Matter **22** (2010) 176003 (6pp) doi:10.1088/0953-8984/22/17/176003

Orbital dilution effect in ferrimagnetic $Fe_{1-x}Mn_xCr_2O_4$: competition between anharmonic lattice potential and spin–orbit coupling

S Ohtani, Y Watanabe, M Saito, N Abe, K Taniguchi, H Sagayama, T Arima[1], M Watanabe and Y Noda

Institute of Multidisciplinary Research for Advanced Materials, Tohoku University, Sendai 980-8577, Japan

E-mail: arima@tagen.tohoku.ac.jp

Received 1 February 2010, in final form 18 March 2010
Published 12 April 2010
Online at stacks.iop.org/JPhysCM/22/176003

Abstract

Magnetic and structural phase diagram in a spinel-type solid solution system $Fe_{1-x}Mn_xCr_2O_4$ has been investigated. The cubic-to-tetragonal transition temperature T_{s1} is gradually reduced by the substitution of Mn^{2+} ($3d^5$) for Jahn–Teller-active Fe^{2+} ($3d^6$) ions, implying the long-range nature of the ferroic interaction between orbitals. In the paramagnetic tetragonal phase for $x < 0.5$, the c parameter is shorter than a because of the anharmonicity of the elastic energy. The crystal structure further changes to orthorhombic at around the ferrimagnetic transition temperature T_{N1}. T_{s1} and T_{N1} meet at $x = 0.5$, and Mn substitution of more than 0.5 gives rise to another tetragonal phase with $a < c$. The systematic change in crystal structure is discussed in terms of competition between the anharmonic lattice potential and the intra-atomic spin–orbit interaction at Fe^{2+}.

(Some figures in this article are in colour only in the electronic version)

1. Introduction

The orbital degree of freedom in 3d transition-metal compounds plays a key role in their physical properties. In particular, the effect of orbital degeneracy on the crystal structure of transition-metal compounds has long been discussed [1–6]. When the electronic orbital levels of transition-metal ions are degenerate, the cooperative Jahn–Teller effect generally causes the spontaneous crystal distortion [7]. Many studies have been performed on spinel-type transition-metal oxides such as $CuFe_2O_4$, Mn_3O_4, $FeCr_2O_4$, $NiCr_2O_4$ and $CuCr_2O_4$, in which the crystal structure is cubic at high temperatures. For instance, in an inverse spinel $CuFe_2O_4$, the Jahn–Teller distortion relevant to the d_γ orbitals of Cu^{2+} ions at octahedral sites causes a structural transition from cubic to tetragonal at ∼630 K [8]. A similar tetragonal distortion is observed in Mn_3O_4 with Jahn–Teller-active Mn^{3+} ions at octahedral sites. In these compounds, the twofold d_γ level of Cu^{2+} and Mn^{3+} is split with the elongated tetragonal distortion. Öpik and Pryce pointed out that the elongated character of the stable distortion should originate from the anharmonic terms of the elastic energy [9][2]. $FeCr_2O_4$ is another typical cooperative Jahn–Teller system with the spinel structure. Fe^{2+} ions with the high-spin $3d^6$ configuration selectively occupy tetrahedral sites. One electron of the minority spin therefore occupies the lower-lying twofold d_γ level. The orbital degree of freedom of the electron causes cooperative Jahn–Teller distortion below 135 K [6]. The compressed tetragonal character ($c < a$) of the low-temperature phase is also attributable to the

[1] Author to whom any correspondence should be addressed.

[2] Liehr and Ballhausen proposed that one should add the second-order contributions of the nuclear displacements to the Jahn–Teller coupling. See [10].

lattice anharmonicity[3] [9]. For such cooperative Jahn–Teller distortion, there would appear to be an infinity of distortions minimizing the free energy without the anharmonic elastic terms. The type of distortion can therefore be modified by some perturbation competing with the lattice anharmonicity, which may provide a good opportunity to develop an exotic function of matter.

In this paper, we report the effect of orbital dilution in the spinel-type $Fe_{1-x}Mn_xCr_2O_4$ system. The substitution of Mn for Fe is regarded as the introduction of voids in terms of orbital degree of freedom, because the high-spin Mn^{2+} ion has no minority-spin electron. The spin sector, by contrast, is expected to be less affected by the substitution, because of a rather small difference in the formal magnetic moment between Fe^{2+} (4 μ_B) and Mn^{2+} (5 μ_B). Furthermore, similar successive magnetic transitions have been reported for $FeCr_2O_4$ and $MnCr_2O_4$ [11–13]. Present measurements of magnetic and structural properties in the solid solution show that the orbital dilution not only reduces the structural transition temperature but also affects the type of cooperative Jahn–Teller distortion. The observed change in distortion type is discussed from the viewpoint of a competition between the lattice anharmonicity and the spin–orbit coupling.

2. Experimental details

Polycrystalline $Fe_{1-x}Mn_xCr_2O_4$ samples were prepared by solid state reaction. Stoichiometric amounts of FeO, MnO and Cr_2O_3 powders were weighed and thoroughly mixed. The mixture was reacted at 900 °C, pressed into a pellet and sintered in an $H_2(1\%)/N_2$ atmosphere at 1350 °C for 24 h. Any impurity phase was not observed in powder x-ray diffraction patterns. Magnetization measurements were carried out in a warming run by using a superconducting quantum interference device (Chimag, Conductus Ltd). High-resolution x-ray diffraction patterns were collected by using diffractometers on beamlines 4C and 1A at the Photon Factory, Japan.

3. Magnetic and structural properties

Figure 1 gives the temperature dependence of magnetization in an external magnetic field of 10 mT for $0 \leqslant x \leqslant 0.9$. A clear rise in magnetization is observed in every curve. Previous neutron diffraction studies revealed successive magnetic transitions in $FeCr_2O_4$ and $MnCr_2O_4$ [11–13]. Collinear ferrimagnetic order was reported between $T_{N1} \sim 80$ K and $T_{N2} \sim 35$ K for $FeCr_2O_4$ [12]. Similar ferrimagnetic structure is also present in $MnCr_2O_4$ between $T_{N1} \sim 51$ K and $T_{N2} \sim 14$ K [13]. In the ferrimagnetic phases, the Fe or Mn moments align antiparallel to the Cr moments. We may therefore assign the deflection point in each low-field magnetization curve to the ferrimagnetic transition temperature

[3] According to the rule of crystallography, one should rotate the a and b axes by 45° around the c axis to transform the unit cell into a body-centered system when the face-centered cell of a spinel compound is tetragonally distorted. In this paper, however, the cell parameters in tetragonal phases are given for the face-centered tetragonal cell to avoid possible confusion.

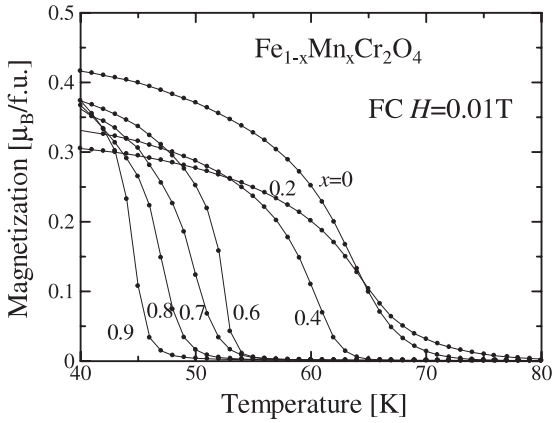

Figure 1. Magnetization of $Fe_{1-x}Mn_xCr_2O_4$ in a magnetic field of 10 mT as a function of temperature. The measurements were performed in a warming run after the samples were cooled in the magnetic field.

T_{N1} for $Fe_{1-x}Mn_xCr_2O_4$. The transition temperature T_{N1} gradually decreases with the Mn substitution. As the temperature further decreases below T_{N2}, incommensurate triple-conical magnetic modulation shows up in $FeCr_2O_4$ and $MnCr_2O_4$ [11–13]. The noncollinear magnetic structure is possibly due to the geometrical frustration in the Cr spin system of the pyrochlore lattice. In the present study, a weak anomaly is found at $T_{N2} = 35$ K in the magnetization data of our $FeCr_2O_4$ sample in 5 T (figure 2(b)), which is attributable to the magnetic transition to the triple cone phase. We assign similar anomalies for the solid solutions (not shown) to the transition to the conical phase, because the spin frustration is essentially irrelevant to the Mn substitution.

Temperature dependence of the x-ray diffraction profile for $x = 0$, 0.4 and 0.7 is shown in figures 2(a), (c) and (e), respectively. The structural transition temperature and the peak splitting are clearly suppressed as x increases. In $FeCr_2O_4$, the (800) peak begins splitting at around $T_{s1} \sim 140$ K, indicating the cooperative Jahn–Teller distortion related to a ferroic arrangement of occupied d_γ orbitals of Fe^{2+}. T_{s1} for $x = 0.4$ and 0.7 are approximately 80 K and 50 K, respectively. The lower-angle peak in figure 2(a) shows a further small split at $T_{s2} \sim T_{N1} \sim 70$ K, indicating another structural transition from tetragonal to orthorhombic. The peak splitting becomes larger with the 40% Mn substitution, while the tetragonal splitting becomes smaller as shown in figures 2(c) and (d). In $Fe_{0.3}Mn_{0.7}Cr_2O_4$, which exhibits a cubic-to-tetragonal transition at a lower temperature than the ferrimagnetic transition temperature, tetragonal distortion of an elongated type ($a < c$) is observed and the low-temperature orthorhombic phase is absent.

4. Phase diagram

The phase diagram of $Fe_{1-x}Mn_xCr_2O_4$ is summarized in figure 3. The cubic-to-tetragonal structural transition temperature T_{s1} shown by solid circles decreases as the Mn^{2+} concentration increases. Here it is interesting to

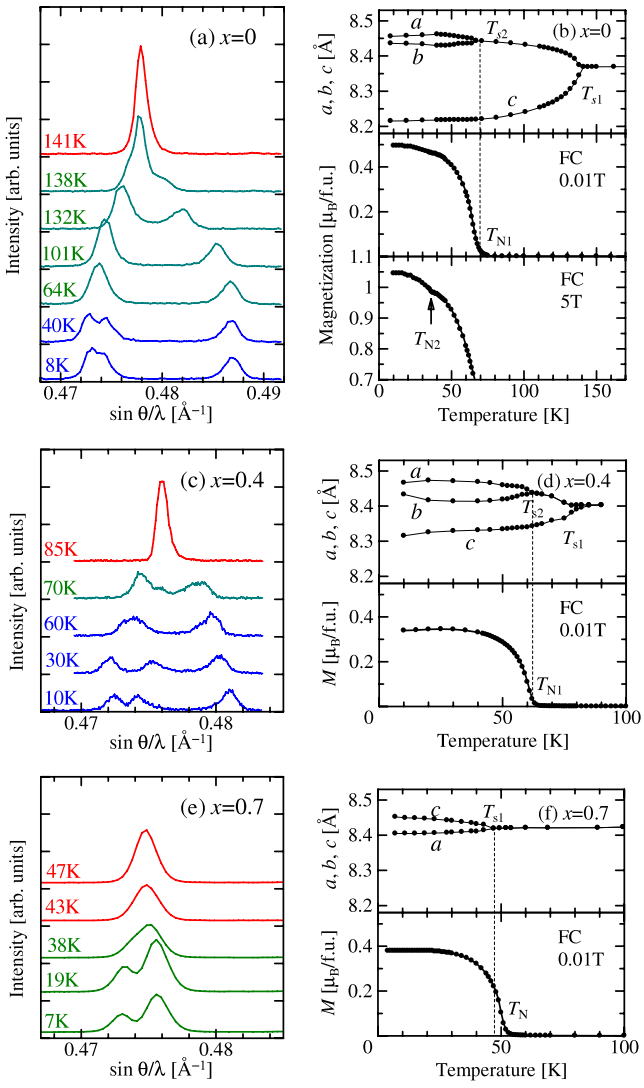

Figure 2. Temperature dependence of the profile of x-ray (800) diffraction in the cubic setting, lattice parameters and magnetization of $Fe_{1-x}Mn_xCr_2O_4$ with ((a), (b)) $x = 0$, ((c), (d)) $x = 0.4$, and ((e), (f)) $x = 0.7$.

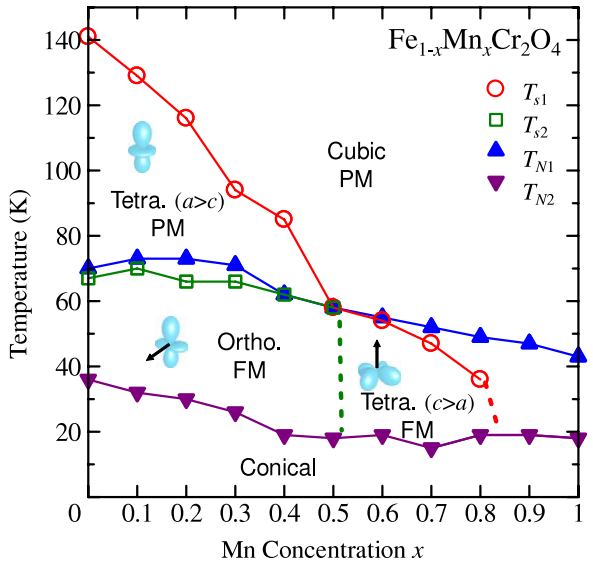

Figure 3. Phase diagram of $Fe_{1-x}Mn_xCr_2O_4$. PM: paramagnetic phase. FM: ferrimagnetic phase. Tetragonal (Tetra.) and orthorhombic (Ortho.) phases are accompanied by Fe^{2+} orbital ordering shown by schematic drawing. Arrows attached to 3d orbital indicate the Fe^{2+} spin orientations. The data for $x = 1$ are quotes from [11].

compare the observed orbital dilution effect with the well-known spin-dilution effect in a ferromagnet. A Monte Carlo calculation showed that the site-percolation limit for the diamond lattice is approximately 0.43 [14]. Although Fe^{2+} and Mn^{2+} ions form the diamond lattice in the spinel-type $Fe_{1-x}Mn_xCr_2O_4$, the cubic–tetragonal transition survives for the orbital concentration at least down to $1 - x = 0.2$, which is much *smaller* than the percolation limit. T_{s1} is roughly proportional to the Fe concentration $1 - x$, in accordance with the mean-field theory. This implies the long-range coupling between Fe^{2+} d_γ orbitals via a strain field in the spinel system, where FeO_4 tetrahedra are isolated from one another [5, 15]. It is worth noting that, in another orbital diluted system $KCu_{1-x}Zn_xF_3$, the critical concentration for the cooperative Jahn–Teller distortion has been found to be around $1 - x = 0.6$ [16]. This value is a bit *larger* than the percolation limit for the simple cubic lattice, 0.31 [14]. The contrast between the two orbital-dilute systems may be caused by the different orbital interactions. In a distorted perovskite $KCuF_3$, Cu^{2+} ions with $3d^9$ form a pseudo-cubic lattice. Each fluorine ion is located close to the midpoint of two Cu ions. The stretching type of distortion of the Cu–F bonds can lead to the antiferroic interaction between the orbitals on two adjacent Cu ions. The short-range nature of the orbital interaction makes the critical concentration much smaller than the present $Fe_{1-x}Mn_xCr_2O_4$ case, where two adjacent Fe sites are not directly linked by an anion.

The ferrimagnetic transition temperature T_{N1} and the conical magnetic transition temperature T_{N2} are less sensitive to the Mn substitution than the structural transition temperature T_{s1}. This is likely due to the small difference in magnetic moment between Fe^{2+} ($S = 2$) and Mn^{2+} ($S = 5/2$). As a result, the structural transition temperature T_{s1} decreases to meet the ferrimagnetic transition temperature T_{N1} at around $x \sim 0.5$.

Figure 3 also suggests a strong coupling between magnetism and structure. It seems that the ferrimagnetic transition accompanies a structural transition for $x < 0.5$. The crystal structure transforms to orthorhombic at $T_{s2} \sim T_{N1}$. A similar orthorhombic distortion was reported in some spinel-type mixed chromites, $Cu_{1-x}Ni_xCr_2O_4$ and $Fe_{1-x}Ni_xCr_2O_4$ [5]. Pure $NiCr_2O_4$ becomes tetragonal with $c > a$ in contrast to $CuCr_2O_4$ and $FeCr_2O_4$ with the spontaneous tetragonal distortion with $c < a$. The orthorhombic distortion in the mixed crystals should originate from the competition between the two types of distortion. In the case of $Fe_{1-x}Mn_xCr_2O_4$, on the other hand, $MnCr_2O_4$ does not contain any Jahn–Teller-active ions. Therefore, the origin of the orthorhombic distortion should be different from that in $Cu_{1-x}Ni_xCr_2O_4$ and $Fe_{1-x}Ni_xCr_2O_4$. The orthorhombic distortion in $Fe_{1-x}Mn_xCr_2O_4$ should be ascribed

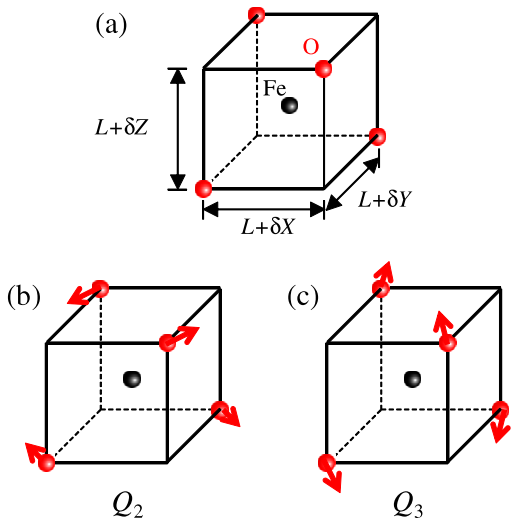

Figure 4. Two Jahn–Teller distortion modes of an FeO_4 tetrahedron. (a) Description of the distortion by using δX, δY and δZ. (b) Normal mode Q_2. (c) Normal mode Q_3.

to the interplay between spin and orbital at the Fe^{2+} ions, as discussed in the next section.

5. Shape of occupied orbital in Fe^{2+} ions

In the following, we discuss how the mean shape of the occupied orbital for a minority-spin electron on each Fe^{2+} ion is affected by the Mn substitution and magnetic ordering. First, we introduce the effective Hamiltonian of the orbital–lattice coupling following Van Vleck [17]. The orbital shape of the d_γ level is represented by a linear combination of two wavefunctions ϕ_1 and ϕ_2, which correspond to $d_{3z^2-r^2}$ and $d_{x^2-y^2}$, respectively. In order to describe the distortion of an FeO_4 tetrahedron, we define the modulation of the dimensions of the cube of edge length L which has four vertices common to the tetrahedron as δX, δY and δZ, as shown in figure 4(a). Two relevant normal distortion modes are then given by

$$Q_2 = \frac{1}{\sqrt{2}L}(\delta X - \delta Y), \tag{1}$$

and

$$Q_3 = \frac{1}{\sqrt{6}L}(2\delta Z - \delta X - \delta Y), \tag{2}$$

which are schematically drawn in figure 4.

In $FeCr_2O_4$, ferroic orbital order is observed below T_{s1}. In such a ferroic orbital-order system, one can consider that the macroscopic distortion should be roughly determined by the average of the local distortion of each polyhedron [4, 5]. Considering that Mn^{2+} ions with the concentration of x are free from any Jahn–Teller instability, we can describe

$$\frac{a-b}{\sqrt{2}\sqrt[3]{abc}} \simeq (1-x)\langle Q_2\rangle, \qquad \frac{2c-a-b}{\sqrt{6}\sqrt[3]{abc}} \simeq (1-x)\langle Q_3\rangle. \tag{3}$$

The effective Hamiltonian for the coupling between the distortion and orbital occupation can be expressed as

$$H_1 = -A_1(\tau_x Q_2 + \tau_z Q_3). \tag{4}$$

Here the Pauli matrix τ is introduced for the two-dimensional space spanned by ϕ_1 and ϕ_2. The Pauli matrix operates as follows:

$$\tau_z\phi_1 = \phi_1, \qquad \tau_z\phi_2 = -\phi_2, \qquad \tau_x\phi_1 = \phi_2, \qquad \tau_x\phi_2 = \phi_1. \tag{5}$$

The coupling constant A_1 is negative for the $Fe^{2+}O_4$ tetrahedron. As a consequence, the orbital shape is deduced from the lattice parameters using equations (4) and (3), assuming the strong interaction between orbital and lattice.

The changes in lattice parameters with Mn substitution for 80 K and 30 K are shown in figures 5(a) and (b), respectively. The crystals are paramagnetic at 80 K, while some magnetically ordered phase is present at 30 K. On increasing Jahn–Teller-inactive Mn^{2+} ions, the lattice distortion reduces, as expected. Simultaneously, the shape of the unit cell at 30 K gradually changes. The average distortion of FeO_4 tetrahedra for 80 K and 30 K is estimated by using equations (3) and plotted in figures 5(c) and (d), respectively. In these figures, we take account of the ambiguity about the definition of the three crystallographic axes. We also attach the orbital shapes predicted in the strong coupling case. The difference between the diagram for 80 K and that for 30 K strongly suggests a strong effect of the magnetic order on the distortion mode. In the paramagnetic phase, the orbital shape is deduced to be of $d_{3z^2-r^2}$ type, irrespective of the orbital dilution. In contrast, the $d_{x^2-y^2}$-type orbital seems stable for the ferrimagnetic state in $0.6 \leqslant x \leqslant 0.8$. Intermediate orbital states are observed in the spin-ordered phase for lower Mn concentrations.

As has been pointed out by Öpik and Pryce [9], an infinite number of distortions would minimize the total of the orbital–lattice coupling given by equation (4) and the harmonic potential energy associated with Q_2 and Q_3. The degeneracy is lifted if the anharmonic term of the elastic potential energy is taken into account. The potential energy V is represented as

$$V = \tfrac{1}{2}M\omega^2 Q^2 + A_3 Q^3 \cos 3\theta + \cdots. \tag{6}$$

Here, Q and θ are the polar coordinates for the two-dimensional Q_2–Q_3 space. In the case of a FeO_4 tetrahedron, the potential energy between neighboring oxygen ions gives positive A_3. Combining equations (4) and (6), Öpik and Pryce showed that three values of θ, $\pi/3$, π and $5\pi/3$, give the ground state [9]. This model explains the distortion in the paramagnetic phase of $Fe_{1-x}Mn_xCr_2O_4$ with $x \leqslant 0.5$ shown in figure 5(c).

We next investigate the origin of the structural change upon the ferrimagnetic phase transition. The result shown in figure 5(d) indicates that $x^2 - y^2$-type orbitals are stabilized in the ferrimagnetic phase for $x \geqslant 0.6$. Generally, the spin–orbit coupling is considered only for the Jahn–Teller distortion associated with d_ε orbitals, as discussed by Kanamori [4], because the first-order perturbation of spin–orbit coupling is absent for the d_γ orbitals. We propose that the second-order term of spin–orbit coupling $\lambda L \cdot S$ would affect the orbital shape. Suppose that an Fe^{2+} ion is in a positive molecular field $H_{\rm eff}$ along the z axis. When the minority spin (i.e. up-spin)

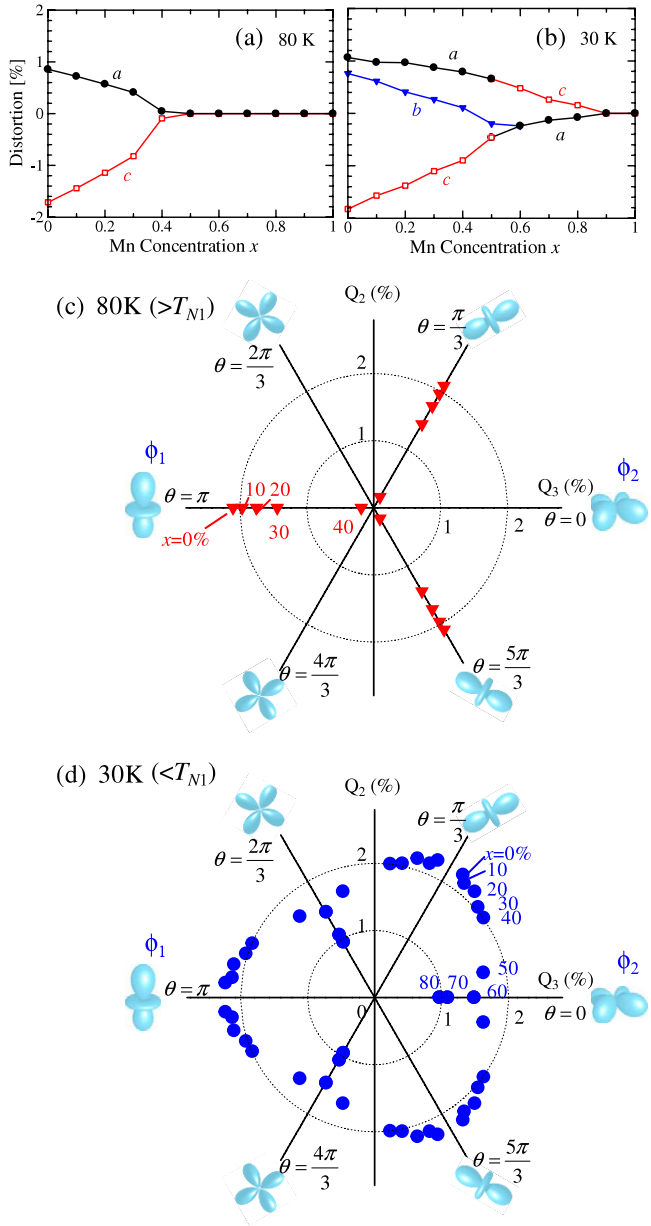

Figure 5. (a), (b) Relative changes of lattice parameters in $Fe_{1-x}Mn_xCr_2O_4$ at (a) 80 K and (b) 30 K. (c), (d) Distortion of the tetrahedron at (c) 80 K and (d) 30 K. The normal modes Q_2 and Q_3 are calculated using equations (3). Average shapes of Fe^{2+} orbital for minority spin predicted from the distortion in the strong lattice–orbital coupling case are also attached (see the text).

occupies the ϕ_1 orbital, the energy gain from the spin–orbit perturbation is calculated to be

$$-\frac{|\langle L_z=-1, S_z=-1|\frac{\lambda}{2}L_-S_+|L_z=0, S_z=-2\rangle|^2}{E(L_z=-1, S_z=-1)-E(L_z=0, S_z=-2)} = -\frac{6\lambda^2}{\Delta+2\mu_B H_{\rm eff}}. \quad (7)$$

Here Δ stands for the ligand field splitting between d_γ and d_ε, and E denotes the energy for the state in the parentheses. When the ϕ_2 orbital is filled, on the other hand, two excited states are hybridized through the spin–orbit coupling. The energy gain from the spin–orbit coupling is thus the summation of

$$-\frac{|\langle L_z=1, S_z=-1|\frac{\lambda}{2}L_-S_+|\phi_2, S_z=-2\rangle|^2}{E(L_z=1, S_z=-1)-E(\phi_2, S_z=-2)} = -\frac{2\lambda^2}{\Delta+2\mu_B H_{\rm eff}}, \quad (8)$$

and

$$-\frac{|\langle xy, S_z=-2|\lambda L_zS_z|\phi_2, S_z=-2\rangle|^2}{E(xy, S_z=-2)-E(\phi_2, S_z=-2)} = -\frac{16\lambda^2}{\Delta}. \quad (9)$$

Comparing the two cases, it is concluded that the spin–orbit term should stabilize ϕ_2 compared to ϕ_1, when the magnetization is parallel to the z axis. The energy difference B (>0) between ϕ_1 and ϕ_2 is roughly proportional to λ^2/Δ.

Applying this result, the effective Hamiltonian $H_{\rm s.o.}$ for the second-order perturbation of the spin–orbit coupling is represented as

$$H_{\rm s.o.} = \frac{B}{6}((3S_z^2-S^2)\tau_z - \sqrt{3}(S_x^2-S_y^2)\tau_x). \quad (10)$$

This effective Hamiltonian evidently stabilizes the deformation of FeO_4 with $\theta = 0, 2\pi/3$ and $4\pi/3$ and hence competes with the anharmonic term of the lattice potential $A_3Q^3\cos 3\theta$. On decreasing the concentration of orbital active Fe^{2+} ions, the amplitude of distortion is reduced and the anharmonic term becomes less important. In comparison, Mn substitution has a limited impact on the intra-atomic spin–orbit term. As a result, the θ value goes to 0. When the magnetization direction is parallel to the x or y axes, $d_{y^2-z^2}$ or $d_{z^2-x^2}$ orbitals become stable. The variation of θ with x at 30 K shown in figure 5(d) is well explained by this model.

6. Summary

We have investigated the structure and magnetism in $Fe_{1-x}Mn_xCr_2O_4$. The substitution of Mn^{2+} for Fe^{2+} reduces the cubic-to-tetragonal transition temperature T_{s1}, as expected. The gradual decrease in T_{s1} with increasing Mn^{2+} is likely due to the long-range nature of the orbital–orbital interaction via distortion.

A systematic change in the crystal structure with temperature and composition is found. Tetragonal distortion with $c < a$ is found for the paramagnetic phase of the $x < 0.5$ compounds, which is attributable to the anharmonic elastic energy. The magnetic-order transforms the compressed tetragonal distortion into the orthorhombic or elongated tetragonal distortion. The behavior can be explained in terms of the competition between the lattice anharmonicity and the intra-atomic spin–orbit interaction.

Acknowledgments

The authors are grateful to S Konno, H Umetsu and H Sawa for their help in sample preparation and synchrotron x-ray measurements. Discussions with S Ishihara were fruitful. This work was partly supported by Grants-In-Aid for Scientific Research (nos. 19340089 and 19052001) from JSPS and MEXT, Japan.

References

[1] Goodenough J B and Loeb A L 1955 *Phys. Rev.* **98** 391
[2] Goodenough J B 1955 *Phys. Rev.* **100** 564
[3] Dunitz J D and Orgel L E 1957 *J. Chem. Phys. Solids* **3** 20
[4] Kanamori J 1960 *J. Appl. Phys.* **31** (Suppl.) S14
[5] Kataoka M and Kanamori J 1972 *J. Phys. Soc. Japan* **32** 113
[6] Wold A, Arnott R J, Whipple E and Goodenough J B 1963 *J. Appl. Phys.* **34** 1085
[7] Jahn H A and Teller E 1937 *Proc. R. Soc.* A **161** 220
[8] Ohnishi H, Teranishi T and Miyahara W 1959 *J. Phys. Soc. Japan* **14** 106
[9] Öpik U and Pryce M H L 1957 *Proc. R. Soc.* A **238** 425
[10] Liehr A D and Ballhausen C J 1958 *Ann. Phys.* **3** 304
[11] Hastings J M and Corliss L M 1962 *Phys. Rev.* **126** 556
[12] Shirane G, Cox D E and Pickart S J 1964 *J. Appl. Phys.* **35** 954
[13] Tomiyasu K, Fukunaga J and Suzuki H 2004 *Phys. Rev.* B **70** 214434
[14] Frisch H L, Hammersley J M and Welsh D J A 1962 *Phys. Rev.* **126** 949
[15] Terauchi H, Mori M and Yamada Y 1972 *J. Phys. Soc. Japan* **32** 1049
[16] Tatami N, Ando Y, Niioka S, Kira H, Onodera M, Nakao H, Iwasa K, Murakami Y, Kakiuchi T, Wakabayashi Y, Sawa H and Itoh W 2007 *J. Magn. Magn. Mater.* **310** 787
[17] Van Vleck J H 1939 *J. Chem. Phys.* **7** 72